Exact theory of nonlinear *p*-polarized optical waves

A. D. Boardman
Department of Physics, University of Salford, Salford M5 4WT, United Kingdom

A. A. Maradudin
Department of Physics, University of California, Irvine, California 92717

G. I. Stegeman
Optical Sciences Center, University of Arizona, Tuscon, Arizona 85721

T. Twardowski
Department of Physics, University of Salford, Salford M5 4WT, United Kingdom

E. M. Wright
Optical Sciences Center, University of Arizona, Tuscon, Arizona 85721
(Received 30 June 1986)

Exact calculations are presented of the properties of nonlinear *p*-polarized waves propagating along the plane boundary between a nonabsorbing, optically self-focusing, nonlinear dielectric and a nonabsorbing positive, or negative, linear dielectric. A nonlinear polarization is used that arises from a number of causes for both Kerr-like and non-Kerr-like saturating media. In the results given here the linear dielectric is a metal, if negative, and is glass if positive. It is found that the variation of the power flow along the guiding surface with effective index, for negative linear dielectrics, will always exhibit a maximum. For data corresponding to copper bounded by, for instance, a self-focusing nonlinear semiconductor, access to this maximum involves such a large change in the refractive index of the nonlinear material, that it is of no practical interest. In the visible better matching of the metal to a nonlinear material can, in principle, be achieved so this maximum may be reached for fairly modest nonlinear changes in the refractive index. A detailed comparison is made with approximations that are based upon a curtailed form of nonlinearity. At low frequencies, for modest nonlinear changes in the refractive index, the dependence of the power flow curve upon the effective guide index is fairly close to several of the earlier published theories. These include a well-known approximation in which the transverse field component is assumed to be dominant. The neighborhood of the maximum, and beyond, becomes accessible at higher operating frequencies and significant differences from earlier approximations may then occur. For positive linear dielectrics the exact theory shows a strong similarity to many more approximate ones, as expected, but the difference between the TM and TE surface wave behavior cannot be discounted. We present several sample calculations of the power flow together with detailed plots of the field components, the magnitude of the nonlinearity, the effect of nonlinearity, and the behavior of the first integral.

INTRODUCTION

During the recent upsurge of interest in nonlinear optical wave propagation in planar[1–7] and optical fiber[8] structures there has been a heavy emphasis on TE waves. For these, confidence can be placed in the form of nonlinear dielectric tensors used because, as was first shown a long time ago[2,9,10] the TE nonlinear differential equation for the electric field component has an elegant and exact analytical solution. This fact enables many benchmarks to be developed of both an analytical and numerical kind and encourages detailed solutions. For TM waves, however, the situation is quite different. For these types of nonlinear waves, as has been discussed recently,[11] a number of approximations[11–24] have been employed that limit the applicability of the results, quite often in a spectacular manner. This development has taken place against a background that contains a fairly old exact analytical calculation of the first integral of the guided-wave TM nonlinear equations.[25] The latter was obscurely presented, however, and in a context that is difficult to relate to in optics. It has, therefore, remained unexploited in the modern literature. The discussion of the relative importance of TM waves and whether their behavior can, in certain circumstances, be trivially inferred from the known behavior of TE waves, will be deferred until later in this article.

THEORY

For an isotropic material the nonlinear polarization can be expressed in terms of the fourth-rank susceptibility tensor X_{ijkl} which has 21 nonzero elements of which only three are independent:

$$\chi_{ijkl}=\chi_{1122}\delta_{ij}\delta_{kl}+\chi_{1212}\delta_{ik}\delta_{jl}+\chi_{1221}\delta_{il}\delta_{jk} \; . \tag{1}$$

For TM waves propagating in the x direction and in the x-z plane, only field components E_x and E_z need to be considered, and in these waves E_x and E_z are $\pi/2$ out of phase.[22,26] The nonlinear polarization for wave mixing in which the frequency remains the same is[27]

$$P_i=2\epsilon_0\chi_{1122}E_iE_jE_j^*+\epsilon_0\chi_{1221}E_jE_jE_i^* \; , \tag{2}$$

so that, for guided TM waves the x component of $\mathbf{P}$ is

$$P_x=2\epsilon_0\chi_{1122}\left[1+\frac{\chi_{1221}}{2\chi_{1122}}\right] \times\left[|E_x|^2+\left[\frac{1-\dfrac{\chi_{1221}}{2\chi_{1122}}}{1+\dfrac{\chi_{1221}}{2\chi_{1122}}}\right]|E_z|^2\right]E_x \; . \tag{3}$$

The ratio χ_{1221}/χ_{1122} takes on different values depending upon the nature of the polarization. These are (a) electronic distortion (E): $\chi_{1221}/\chi_{1122}=1$; (b) molecular orientational Kerr effect (M): $\chi_{1221}/\chi_{1122}=6$; and (c) electrostriction and heating (T): $\chi_{1221}=0$.

The components of the nonlinear polarization are, in general form,

$$P_x \propto (|E_x|^2+\gamma|E_z|^2)E_x \; , \tag{4}$$

$$P_z \propto (|E_z|^2+\gamma|E_x|^2)E_z \; , \tag{5}$$

where $\gamma=\frac{1}{3}$, $-\frac{1}{2}$, or 1 according to whether the nonlinear mechanism is (a), (b), or (c).

In this paper all of these mechanisms are assessed, within a local approximation. The nonlinear guided TM waves are characterized by the 2×2 subtensor[22]

$$\epsilon^{TM}=\begin{bmatrix}\epsilon+\alpha_{xx}|E_x|^2+\alpha_{xz}|E_z|^2 & 0\\ 0 & \epsilon+\alpha_{zz}|E_z|^2+\alpha_{zx}|E_x|^2\end{bmatrix} , \tag{6}$$

where ϵ is the linear part of the dielectric function. This generic form of dielectric subtensor is related to the nature of the nonlinear mechanism, and also to some previously published approximations, in the following way: (a) electronic distortion (E): $\alpha_{xx}=\alpha_{zz}=\alpha$, $\alpha_{xz}=\alpha_{zx}=\alpha/3$; (b) molecular orientation (M): $\alpha_{xx}=\alpha_{zz}=\alpha$, $\alpha_{xz}=\alpha_{zx}=-\alpha/2$; (c) electrostriction or thermal (T): $\alpha_{xx}=\alpha_{zz}=\alpha_{xz}=\alpha_{zx}=\alpha$; (d) uniaxial approximation (U_1): $\alpha_{zz}=\alpha$, $\alpha_{xx}=\alpha_{xz}=\alpha_{zx}=0$; (e) uniaxial approximation (U_2): $\alpha_{xx}=\alpha$, $\alpha_{zz}=\alpha_{xz}=\alpha_{zx}=0$; and

$$\alpha=2\chi_{1122}\left[1+\frac{\chi_{1221}}{2\chi_{1122}}\right] . \tag{7}$$

Note that α is often written[22,26] as $\alpha=2\sqrt{\epsilon}n_{2E}$, where the nonlinear refractive index n is related to $|\mathbf{E}|^2$ through $n=\sqrt{\epsilon}+n_{2E}|\mathbf{E}|^2$.

From Maxwell's equations, for a TM guided wave traveling down the x axis with wave number k and angular frequency ω, the basic equations are

$$\frac{\partial E_x}{\partial z}=ikE_z+i\omega\mu_0H_y \; , \tag{8}$$

$$\frac{\partial H_y}{\partial z}=i\omega\epsilon_0\epsilon_{xx}E_x \; , \tag{9}$$

$$ikH_y=-i\omega\epsilon_0\epsilon_{zz}E_z \; . \tag{10}$$

Since, as emphasized above, E_x and E_z are $\pi/2$ out of phase, we can write $E_x=A_x$, $E_z=-iA_z$, and $H_y=-ih_y$, where A_x, A_z, and h_y are real. Hence the basic equations can be reexpressed as

$$\frac{\partial A_x}{\partial Z}=\frac{L}{1-Z}(kA_z+\omega\mu_0h_y) \; , \tag{11}$$

$$\frac{\partial h_y}{\partial Z}=\frac{L}{1-Z}(-\omega\epsilon_0\epsilon_{xx}A_x) \; , \tag{12}$$

$$\frac{\partial A_z}{\partial Z}=\frac{L}{1-Z}\left[\frac{k\epsilon_{xx}A_x-(kA_z+\omega\mu_0h_y)\dfrac{\partial\epsilon_{zz}}{\partial A_z}}{\epsilon_{zz}+A_z\dfrac{\partial\epsilon_{zz}}{\partial A_z}}\right] , \tag{13}$$

$$\frac{\partial \mathscr{P}}{\partial Z}=\frac{L}{1-Z}A_zh_y \; , \tag{14}$$

where μ_0 is the permeability of free space, $\mathscr{P}$ is the power flow down the guide, $Z=1-\exp(-z/L)$, and L is a scaling factor. Note that the transformation converts the range $0<z<\infty$ to $0<Z<1$—a very important step in the numerical work.

The field equations are expressed in the form (11)—(14) in order to use a finite-element general purpose code called COLSYS.[28] The transformation that we considered necessary renders the equations indeterminate at $Z=1$. However, the solution of the nonlinear equations becomes virtually linear in the neighborhood of $Z=1$, and by choosing L so that the linear solution is of the form $A_x=A_0(1-Z)$ we can evaluate the equations by simple linear interpolation. Since the linear solution has the form $\exp(-\kappa z)$, where $\kappa^2=k^2-\omega^2\epsilon/c^2$, then L should be set equal to $1/\kappa$.

The guiding system considered in this paper consists of an interface separating a semi-infinite linear substrate from a semi-infinite nonlinear cladding or superstrate. The substrate may have either a negative or positive dielectric function. The former will be a metal, in this paper, and the latter a substance such as glass. The boundary conditions are

$$A_x(0)=A_0,\quad A_x(1)=h_y(1)=0\ , \tag{15}$$

with A_0 varied until $h_y(0)$ is continuous across the boundary, or

$$h_y(0)=h_0,\quad A_x(1)=h_y(1)=0\ , \tag{16}$$

with h_0 varied until $A_x(0)$ is continuous across the boundary.

In the past the major developments of the theory of p-polarized nonlinear waves have either rested upon two quite different uniaxial assumptions or have assumed a form of nonlinearity that is appropriate to electrostriction or heating.[15,16,23,24] The first uniaxial assumption[12,17] which we label below as U_1 neglects the nonlinearity in the ϵ_{xx} component of the dielectric subtensor and retains only the E_z contribution to the nonlinearity in the ϵ_{zz} component. This assumption is based on the idea that E_z dominates the field of the guided waves in the nonlinear cladding. This only allows the nonlinearity to be effective in the transverse direction. Now it is straightforward to show for the cladding that, in the linear limit, $|E_z/E_x|=(|\epsilon_s/\epsilon_c|)^{1/2}$, where ϵ_c and ϵ_s are, respectively, the cladding and substrate dielectric constants. For the substrate the ratio is inverted. For a metal substrate such as copper that has a large negative dielectric constant, $\epsilon_s=-1000$ at $\lambda\simeq 5.5$ μm, and with InSb as a cladding ($\epsilon_c=16$), it is clear that E_z is indeed dominant. At frequencies in the visible, however, this is not the case and $|E_z/E_x|$ can approach unity. Some minor corrections to the predictions of the U_1 model may be expected, then, in the infrared and major ones are anticipated in the visible.

In the U_2 uniaxial model it is assumed that the nonlinearity is controlled by the E_x component only and it is assumed that ϵ_{zz} has its linear value. For frequencies in the infrared region this virtually eliminates the nonlinearity since it is E_z that is important. The U_2 results in this regime are expected to be locked onto the linear eigenvalue for all reasonable power levels. In the visible region the predictions of the U_2 and the U_1 models are expected to be almost the same since E_x and E_z have equal weight. They will both be significantly different from the exact results, however.

NUMERICAL RESULTS

Figure 1 shows the variation, with effective guide index, of the total power flow along the interface between a metal that has a large negative dielectric constant and a nonlinear cladding with a positive dielectric. Several approximations and the influence of three different types of nonlinearity are contrasted. The wavelength used is in the infrared region and there is a large mismatch between the absolute values of the linear dielectric constants of the two media in contact. The linear eigenvalue, at the zero power level, is a solution of the familiar surface-plasmon polariton dispersion equation.[29] For a practical range of β near the linear eigenvalue, it can be seen that there is little to choose between the various approximations, with the exception of U_2. In this case, as intimated earlier on, the neglect of the strongest field component that contributes to the nonlinearity has made the system essentially linear.

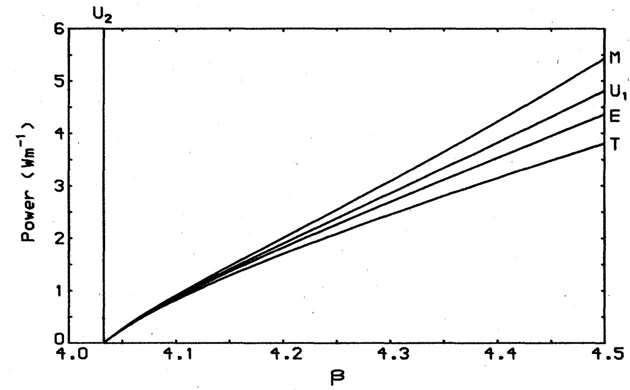

FIG. 1. Total power flow along the interface as function of effective guide index. $\omega=3.425\times10^{14}$ rad s^{-1}. Dielectric constant of the metal is $\epsilon_s=-1000$. Dielectric constant of the nonlinear cladding is $\epsilon_c=16$, $\alpha=4.24\times10^{-9}$ m^2 V^{-2}. $U_{1,2}$ are uniaxial approximations. M, T, and E label molecular orientation Kerr effect, electrostriction (thermal), and nonlinear electronic distortion nonlinearities, respectively.

The power in the U_2 approximation is therefore "locked" onto the linear solution and cannot vary in any detectable way with guide index. The other uniaxial approximation is U_1, and is quite close to the exact case. The variation of total power flow with effective guide index is quite significant compared with the U_2 case, even though the important power range is still fairly close to the coupled-mode regime.

In principle, in Fig. 1, the curves could be extended to very large β and eventually even the U_2 approximation will exhibit a maximum, as all the other curves. This regime can only be reached, as will be seen below, through the generation of enormous unphysical nonlinearities. The visible range of wavelengths is in sharp contrast to this because this maximum can be reached for reasonably modest nonlinear changes in the refractive index. This fact can then be exploited experimentally, provided some reasonable matching of linear index change across the boundary to this nonlinear change can be achieved. In the power curve shown in Fig. 2, the uniaxial approximations

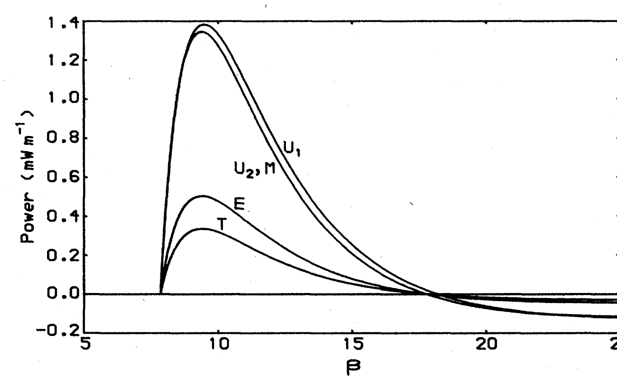

FIG. 2. Total power-flow variation with effective guide index for $\omega=3.66\times10^{15}$ rad s^{-1}, $\epsilon_s=-2.5$, $\epsilon_c=2.405$, and $\alpha=6.4\times10^{-12}$ m^2 V^{-2}. Labels same as for Fig. 1.

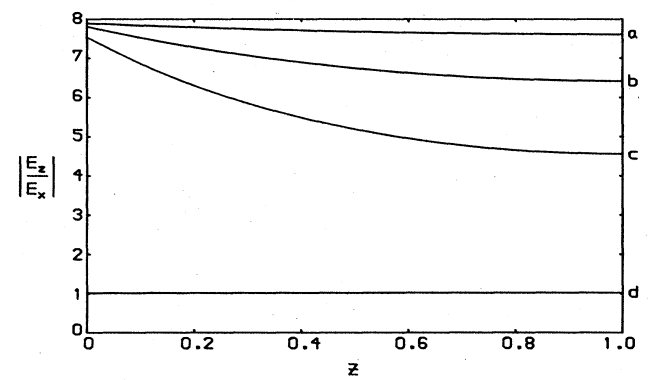

FIG. 3. Variation of the nonlinear cladding-field component ratio with Z for case E with Fig. 1 data: (a) $\beta=4.035$, (b) $\beta=4.05$, and (c) $\beta=4.10$. Figure 2 data: (d) almost independent of β.

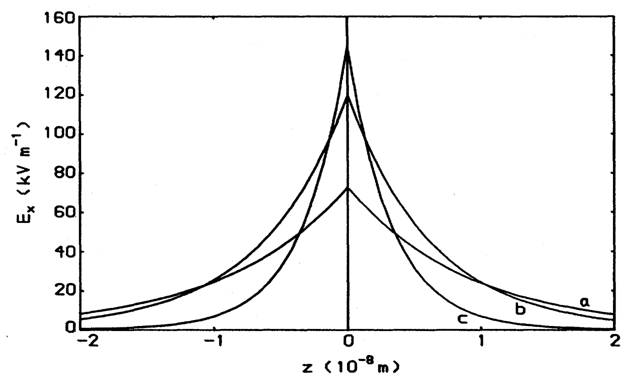

FIG. 5. Variation of E_x with z for the case E with Fig. 2 data. (a) $\beta=9$, (b) $\beta=13$, and (c) $\beta=25$.

are almost indistinguishable from each other and from the curve corresponding to nonlinearity arising from molecular orientation. The curves corresponding to nonlinear electronic distortion and electrostriction have much lower maxima and are fairly close together. In the uniaxial cases the extent of the nonlinear change in the refractive index is underestimated, compared to case E, to almost the same degree. This explains both why they are close together and why they stay close to the linear eigenvalue for longer, as the power changes. Case M, although it is exact, has a negative γ in Eqs. (4) and (5). It therefore involves a smaller effective nonlinearity and thus lies close to the U curves.

Figure 3 shows the Z variation of the ratio of the electric field components in the nonlinear medium for case E. It can be seen that for data corresponding to Fig. 1, a different asymptotic value is reached for each value of β. For data corresponding to Fig. 2, the asymptotic limit is virtually independent of β. This limit has the analytical form

$$\left|\frac{E_z}{E_x}\right|=\frac{\beta}{(\beta^2-\epsilon_c)^{1/2}} . \tag{17}$$

In this formula the β is matched through to the nonlinear region of the interface. It is therefore not the linear value, although (17) has the same form in the linear approximation. The curves (a), (b), and (c) achieve the limits 7.61, 6.45, and 4.56, respectively. For curve (d) the limit is $\simeq 1$ and virtually independent of β.

The nonlinear contribution to the refractive index in the range $0<Z<1$ is presented, for case E, in Fig. 4. For the data corresponding to Fig. 1, it can be seen that as β moves away from the linear eigenvalue an enormous change in the nonlinearity occurs. These changes are unrealizable in real materials and are therefore of academic interest only. The nonlinearity changes from the data of Fig. 2 are within what could be expected for some optically nonlinear substances, even within and beyond the maximum.

Figure 5 displays the variation of the E_x field component across the interface for the case E with the Fig. 2 data set and for a large range of β. At large β in Fig. 2 another curious feature can be seen. This is that the power flow has become negative. Even for linear surface polaritons, the power flow in the medium on either side of the interface is in the opposite direction. At low powers

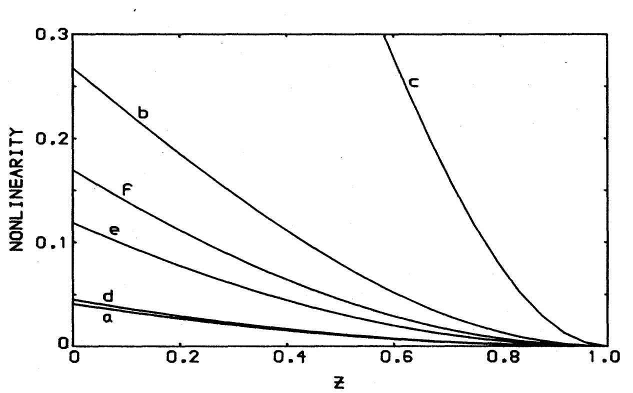

FIG. 4. Nonlinearity as function of Z for case E with Fig. 1 data: (a) $\beta=4.035$, (b) $\beta=4.05$, and (c) $\beta=4.10$. Figure 2 data: (d) $\beta=9$, (e) $\beta=13$, and (f) $\beta=25$.

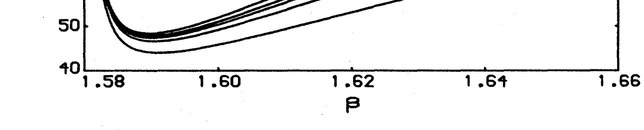

FIG. 6. Total power-flow variation with effective guide index $\omega=3.66\times10^{15}$ rad s^{-1}, cladding dielectric constant $\epsilon_c=2.4025$, $\alpha=6.4\times10^{-12}$ m^{2}V^{-2}. Substrate dielectric constant $\epsilon_s=2.5$. Labels as for Figs. 1 and 2, but S denotes the TE wave case.

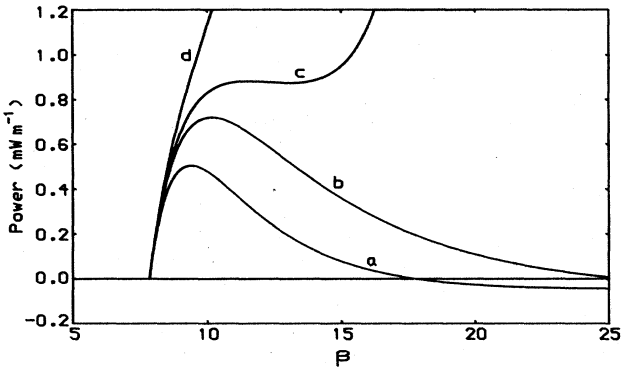

FIG. 7. The effect of saturation on case E of Fig. 2. Maximum nonlinearity: (a) unlimited, (b) 0.10, (c) 0.08, and (d) 0.06.

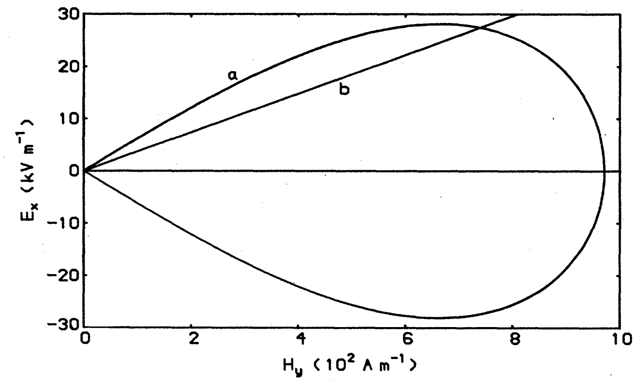

FIG. 8. First integrals. $\beta=1.6$. Data same as for Fig. 6. $E_x=H_y=0$ is at $z=\infty$ and z decreases to zero at the intersection point. (a) Nonlinear cladding; (b) linear substrate.

and in the linear regime this does not provoke any comment since the net flow is positive. In the problem studied here one of the media is now nonlinear. As the value of β increases a strongly nonlinear regime is entered, creating strong powers that are contributed in opposition from each side of the interface. The nonlinearity then causes the net direction to be eventually reversed. Such a situation is likely to be accompanied by high attenuation and saturation effects. This has not been checked here theoretically by actually including absorption, but the inclusion of saturation later on does show that this power flow reversal is opposed.

The case in which the linear dielectric constants on both sides of the interface are both positive is shown in Fig. 6. There is no linear limit for this case and the results exhibit a power threshold, as expected. In fact, this behavior is qualitatively similar to that of TE waves flowing along the interface. In order to make the latter comparison more secure, the power curve for TE waves is also shown in Fig. 6. It can be seen that there is a nontrivial difference in magnitude between the TM cases and the TE case, but the physical behavior is identical. Note that all the reasonable approximations and nonlinear mechanisms for the TM case do not produce results that differ a great deal from each other.

The role of saturation has been neglected up to now but it can be modeled by writing the dielectric tensor elements as

$$\epsilon_{xx}=\epsilon+\alpha_{xx}A^2{}_{xx}\left[1-\exp\left[-\frac{A^2{}_x}{A^2{}_{xx}}\right]\right] +\alpha_{xz}A^2{}_{xz}\left[1-\exp\left[\frac{A^2{}_z}{A^2{}_{xz}}\right]\right], \tag{18}$$

$$\epsilon_{zz}=\epsilon+\alpha_{zz}A^2{}_{zz}\left[1-\exp\left[\frac{A^2{}_z}{A^2{}_{zz}}\right]\right] +\alpha_{zx}A^2{}_{zx}\left[1-\exp\left[\frac{A^2{}_x}{A^2{}_{zx}}\right]\right], \tag{19}$$

where A_{xx}, A_{zz}, A_{zx} and A_{zx} are constants. These equations show that the maximum nonlinearities are

$$\begin{aligned}\epsilon^{NL}{}_{xx,\max}&=\alpha_{xx}A^2{}_{xx}+\alpha_{xz}A^2{}_{xz}\ ,\\ \epsilon^{NL}{}_{zz,\max}&=\alpha_{zz}A^2{}_{zz}+\alpha_{zx}A^2{}_{zx}\ .\end{aligned} \tag{20}$$

This is not the only way to model saturation effects,[23] but it will suffice for the present purpose. Figure 7 shows the role of saturation for the case E with Fig. 2 data. Each curve corresponds to setting all the αA^2 terms in (20) equal to the same value. It is interesting here to see that, apart from the fact that a fairly low value for the maximum achievable nonlinearity will drive the curves toward the linear values, it is possible for media with maximum nonlinearities ≥ 0.1 still to show the maximum in the power curves. This is interesting from the point of view of possible experiment with proof-of-concept materials such as artificial nonlinear dielectrics.[30]

Finally, we show in Fig. 8 the first integrals of the equations for both the linear material and the nonlinear material for $\beta=1.6$ with Fig. 6 data set. These are expressed as a plot of E_x against H_y. The curves intersect at $z=0$, where the boundary exists. They will not be used explicitly in this paper, but such interesting plots will find an eventual use in an analysis of the stability of the nonlinear TM waves.[31] This will be the subject of a forthcoming article.

[1]N. N. Akmediev, Zh. Eksp. Teor. Fiz. **83**, 545 (1982), [Sov. Phys.—JETP **56**, 299 (1982)].
[2]A. A. Maradudin, in *Optical and Acoustic Waves in Solids—Modern Topics,* edited by M. Borissov (World-Scientific, Singapore, 1983).
[3]A. D. Boardman and P. Egan, IEEE J. Quant. Electron. **QE-21**, 1701 (1985).
[4]C. T. Seaton, J. D. Valera, R. L. Shoemaker, G. L. Stegeman,

J. T. Chilwell, and S. D. Smith, IEEE J. Quant. Electron. **QE-21**, 724 (1985).
[5]A. D. Boardman and P. Egan, Philos. Trans. R. Soc. London, Ser. A **313**, 363 (1984).
[6]F. Lederer, U. Langbein, and H.-E. Ponath, Appl. Phys. B **31**, 69 (1983).
[7]D. Mihalache and H. Totia, Rev. Roumaine Phys. **29**, 365 (1984).
[8]A. D. Boardman and G. S. Cooper, Opt. Lett. **11**, 112 (1986).
[9]A. G. Litvak and V. A. Mironov, Izvestiya Vyssh. Uchebn. Zaved. **11**, 1911 (1968).
[10]W. J. Tomlinson, Opt. Lett. **5**, 323 (1980).
[11]A. D. Boardman, G. S. Cooper, P. Egan, and T. Twardowski, in *Optical Bistability III,* edited by H. M. Gibbs, P. Mandel, N. Peyghambarian, and S. D. Smith (Springer-Verlag, Berlin, 1986), pp. 74—78.
[12]G. I. Stegeman and C.T. Seaton, Opt. Lett. **9**, 235 (1984).
[13]A. D. Boardman and P. Egan, J. Phys. (Paris) Colloq. **45**, C5-291 (1984).
[14]V. M. Agranovich, V. S. Babichenko, V. Ya Chernyak, Pis'ma Zh. Eksp. Teor. Fiz. **32**, 532 (1980) [JETP Lett. **32**, 512 (1980)].
[15]K. M. Leung, Phys. Rev. B **32**, 5093 (1985).
[16]N. N. Akmediev, Zh. Eksp. Teor. Fiz. **84**, 1907 (1983) [Sov. Phys.—JETP **57**, 1111 (1983)].
[17]C. T. Seaton, J. D. Valera, B. Svensson, and G. I. Stegeman, Opt. Lett. **10**, 149 (1985).
[18]V. M. Agranovich and V. Ya Chernyak, Solid State Commun. **44**, 1309 (1982).
[19]F. Lederer, U. Langbein, and H.-E. Ponath, Appl. Phys. B **31**, 187 (1983).
[20]D. Mihalche, R. G. Nazmitdinov, and V. K. Fedyanin, Phys. Scr. **29**, 269 (1984).
[21]A. E. Kaplan, Zh. Eksp. Teor. Fiz. **72**, 1710 (1977); [Sov. Phys.—JETP **45**, 896 (1977)].
[22]A. D. Boardman and P. Egan, in Proceedings of the 2nd Conference on Surface Waves on Solid State and Gaseous Plasmas, Ohrid (1985) (World-Scientific, Singapore, in press).
[23]A. Shivarova and N. Dimitrov, Plasma Phys. Contr. Fus. **27**, 219 (1985).
[24]M. Y. Yu, Phys. Rev. A **28**, 1855 (1983).
[25]A. L. Berkhoer and V. E. Zakharov, Zh. Eksp. Teor. Fiz. **58**, 903 (1970); [Sov. Phys.—JETP **31**, 486 (1970)].
[26]G. I. Stegeman, IEEE J. Quant. Electron. **QE-10**, 1612 (1982).
[27]P. D. Maker and R. Terhune, Phys. Rev. **137**, A801 (1964).
[28]U. Ascher, J. Christiansen, and R. D. Russell, ACM Trans. Math. Software **7**, 209 (1981).
[29]A. D. Boardman, in *Electromagnetic Surface Modes,* edited by A. D. Boardman (Wiley, New York, 1982).
[30]P. W. Smith, P. J. Maloney, and A. Ashkin, Opt. Lett. **7**, 347 (1982).
[31]C. T. Jones and J. V. Maloney, in *Optical Bistability III,* Ref. 11, pp. 74—78.